Supplemental figures for Topness et al. Calibration guidelines and a runoff-isotope module for lake proxy system modeling (PRYSM v2.0)

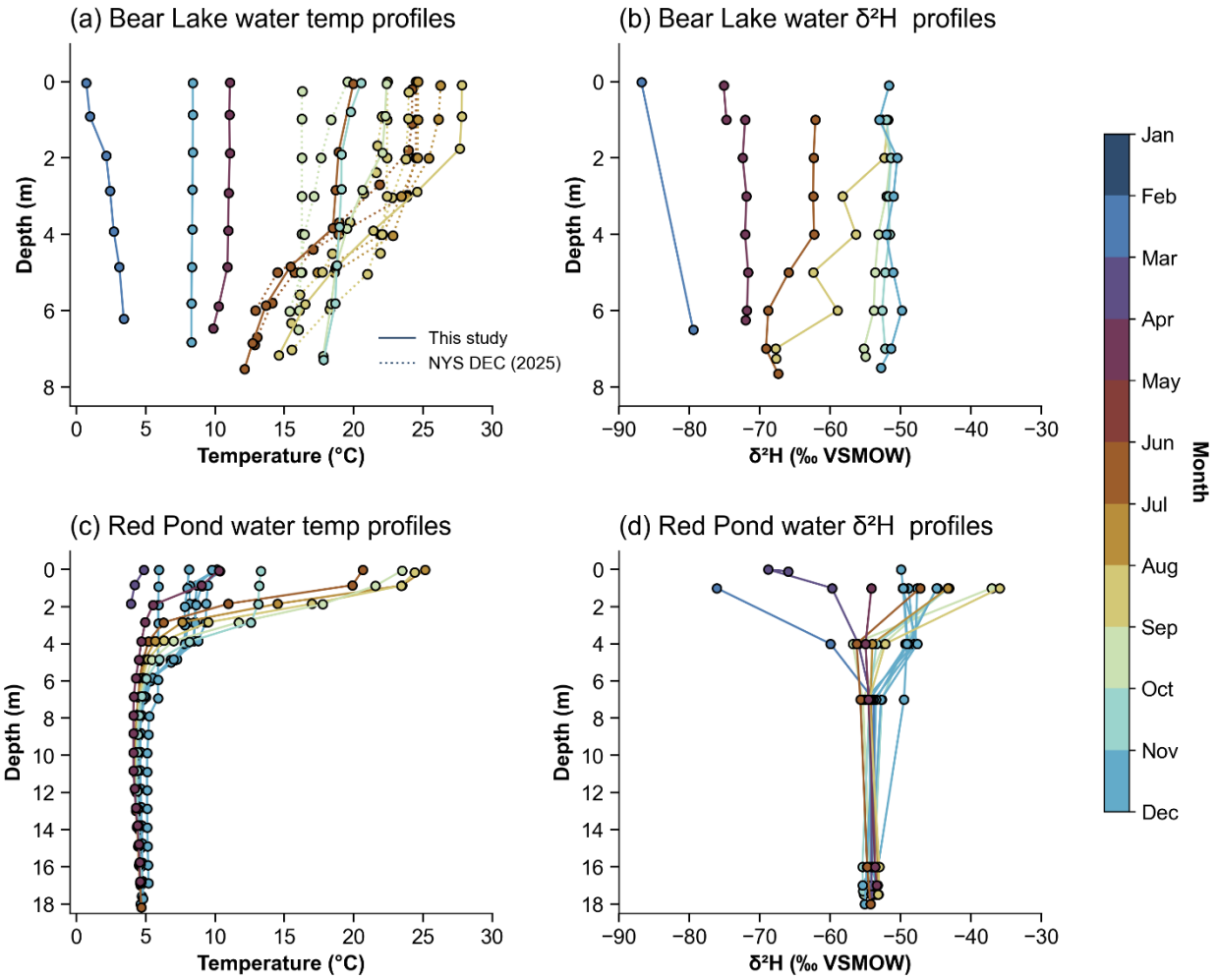

Figure S1. Observed water temperature and water δ^2H profiles for Bear Lake (a-b) and Red Pond (c-d). Profiles are colored by the month they were collected. In panel (a), we show profiles collected during this study (solid lines) and from the New York State Department of Environmental Conservation's Division of Water Monitoring Data Portal (dotted lines; NYS DEC, 2025). Note that water temperature observations from thermistor strings are not shown in this figure.

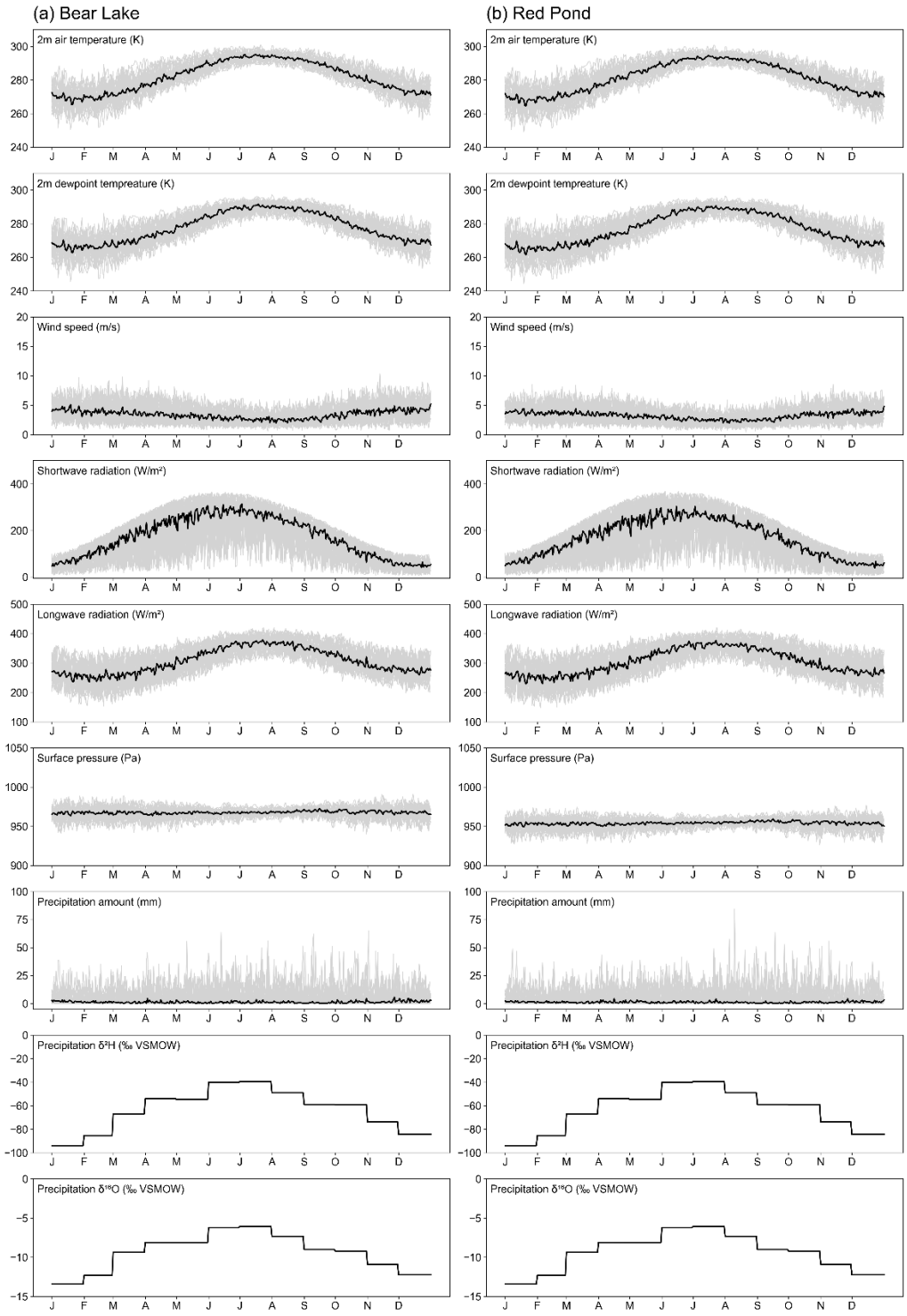

Figure S2. Daily meteorological input variables downloaded from ERA5 Global Reanalysis Data selected for (a) Bear Lake and (b) Red Pond for 1994 to 2025 (Hersbach et al., 2020; Hersbach et al., 2023). Precipitation δ^2H and $\delta^{18}O$ climatologies are observations from Amherst,

New York (Corcoran et al., 2019). Gray lines are individual years and thick black lines show the median over the time interval.

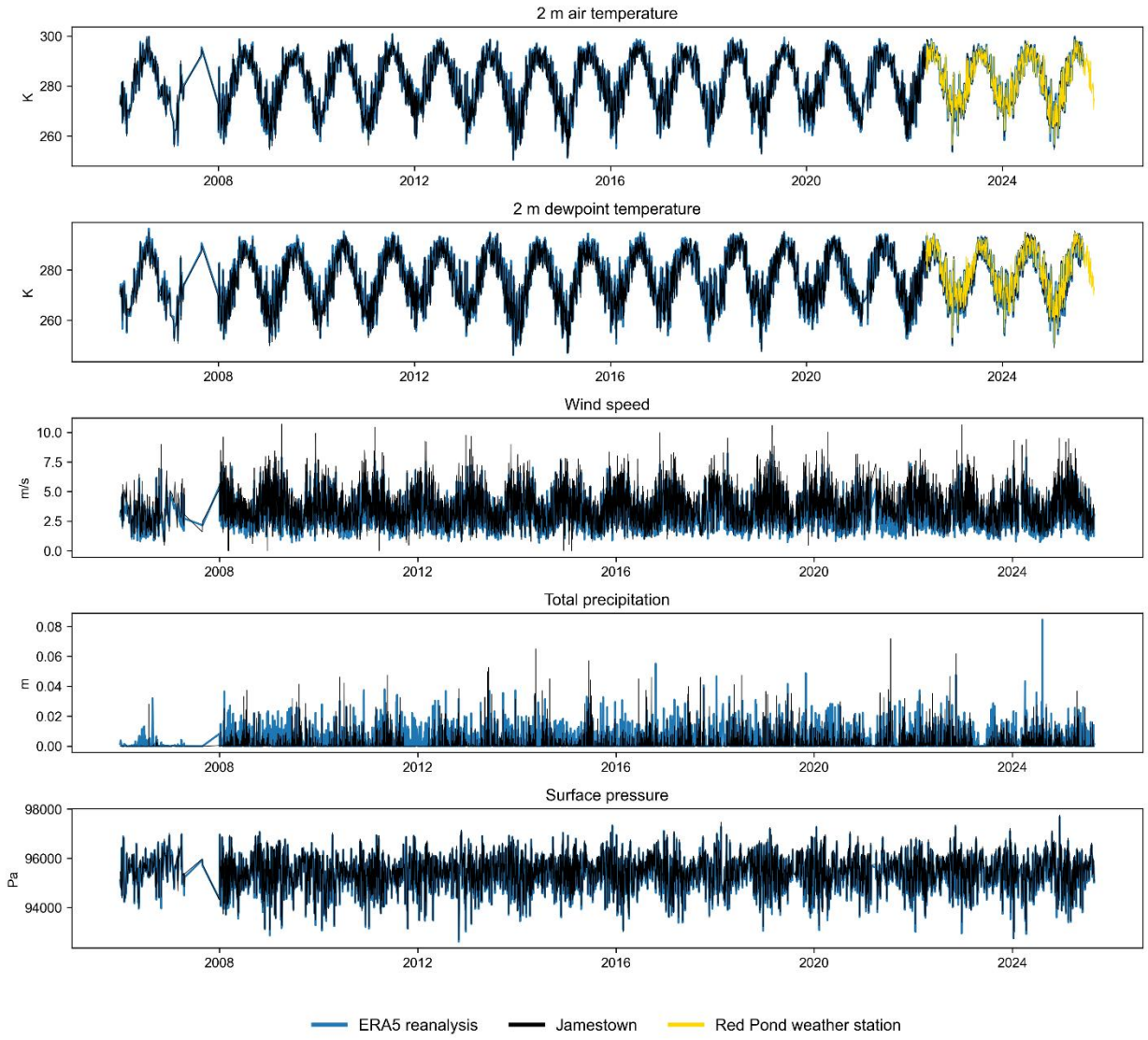

Figure S3. Time series comparison of daily ERA5 Global Reanalysis Data downloaded for Red Pond and observations from weather stations located at Red Pond and Jamestown.

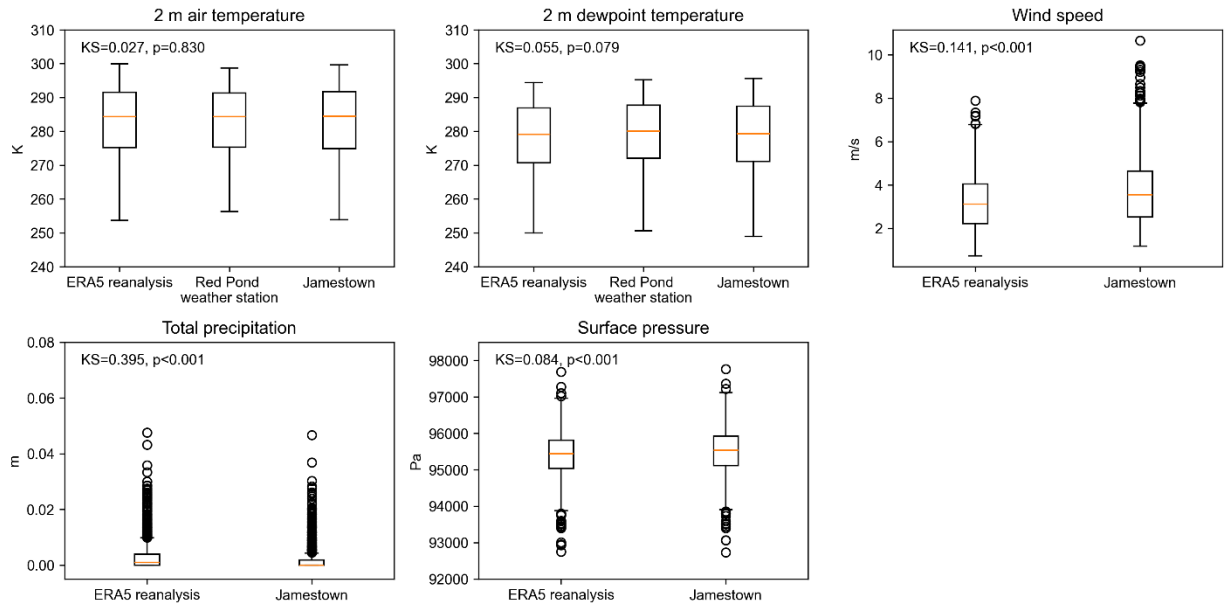

Figure S4. Boxplots comparing daily ERA5 Global Reanalysis Data downloaded for Red Pond and observations from weather stations at Red Pond and Jamestown, New York during June 2022 to November 2025. For each box plot, horizontal lines show the median, the box indicates the 25th to 75th quartile range, and the whiskers display 1.5 times the interquartile range. Outliers are shown as open circles. Kolmogorov-Smirnov (KS) tests and p-values show if differences among ERA5 and Jamestown datasets are significant, except the 2 m air temperature and 2 m dewpoint temperature KS tests and p-values are between ERA5 and the Red Pond weather station data.

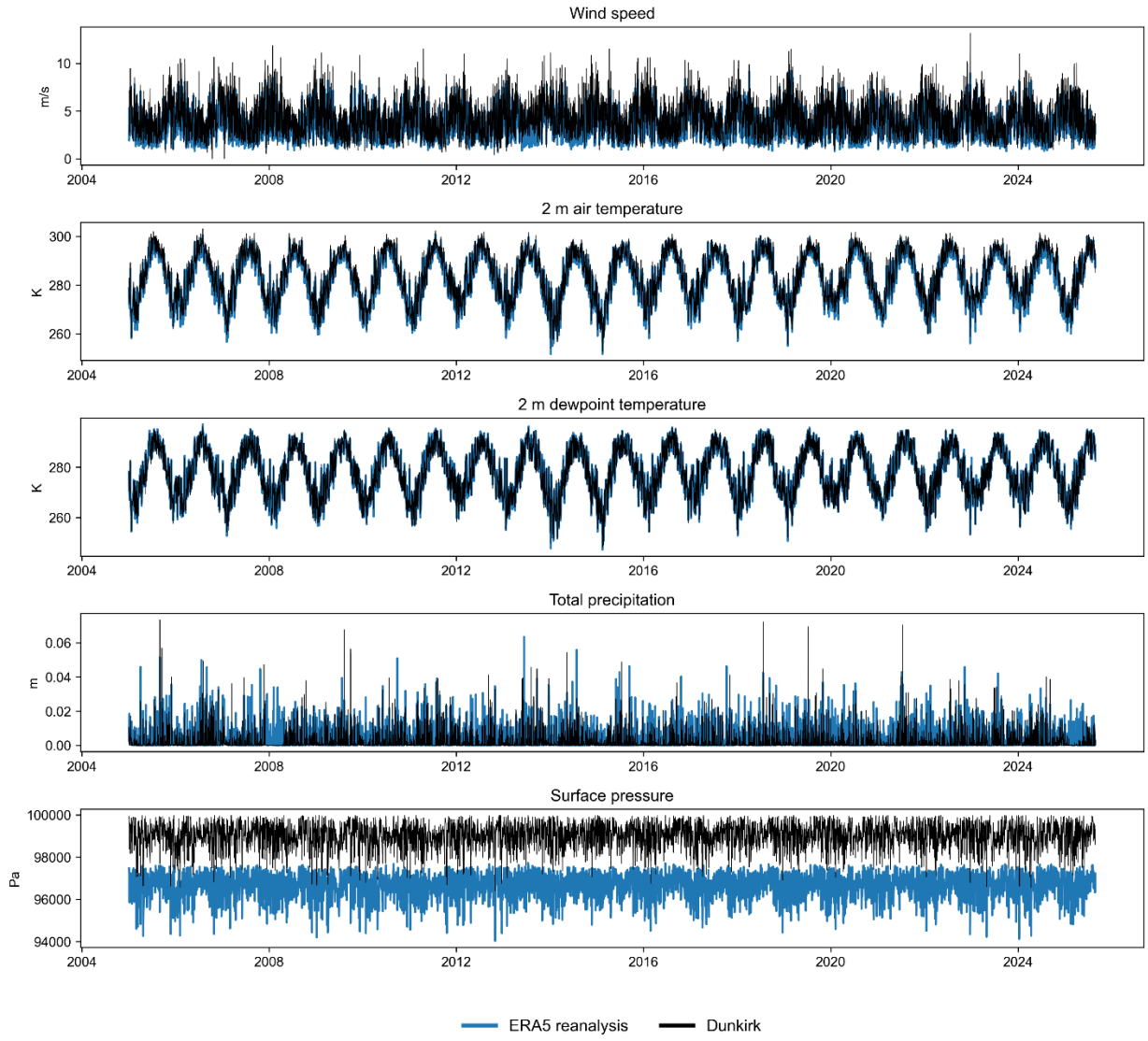

Figure S5. Time series comparison of daily ERA5 Global Reanalysis Data downloaded for Bear Lake and weather station observations from Dunkirk, New York.

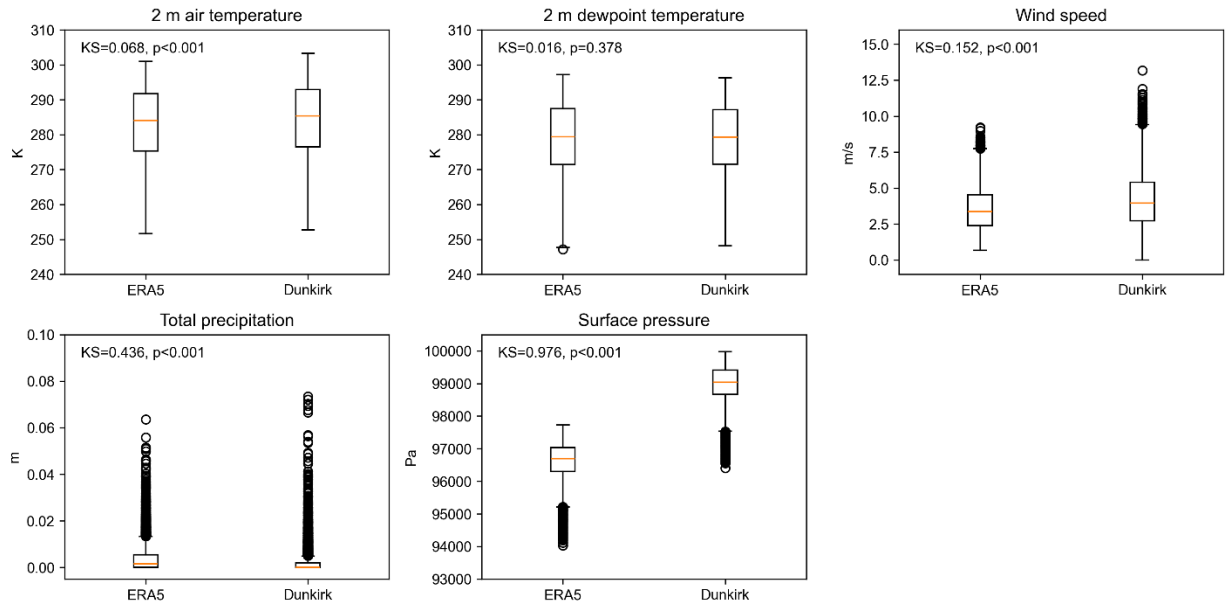

Figure S6. Comparison among daily ERA5 Global Reanalysis Data downloaded for Bear Lake and observations from Dunkirk, New York during January 2005 to August 2025. For each box plot, horizontal lines show the median, the box indicates the 25th to 75th quartile range, and the whiskers display 1.5 times the interquartile range. Outliers are shown as open circles.

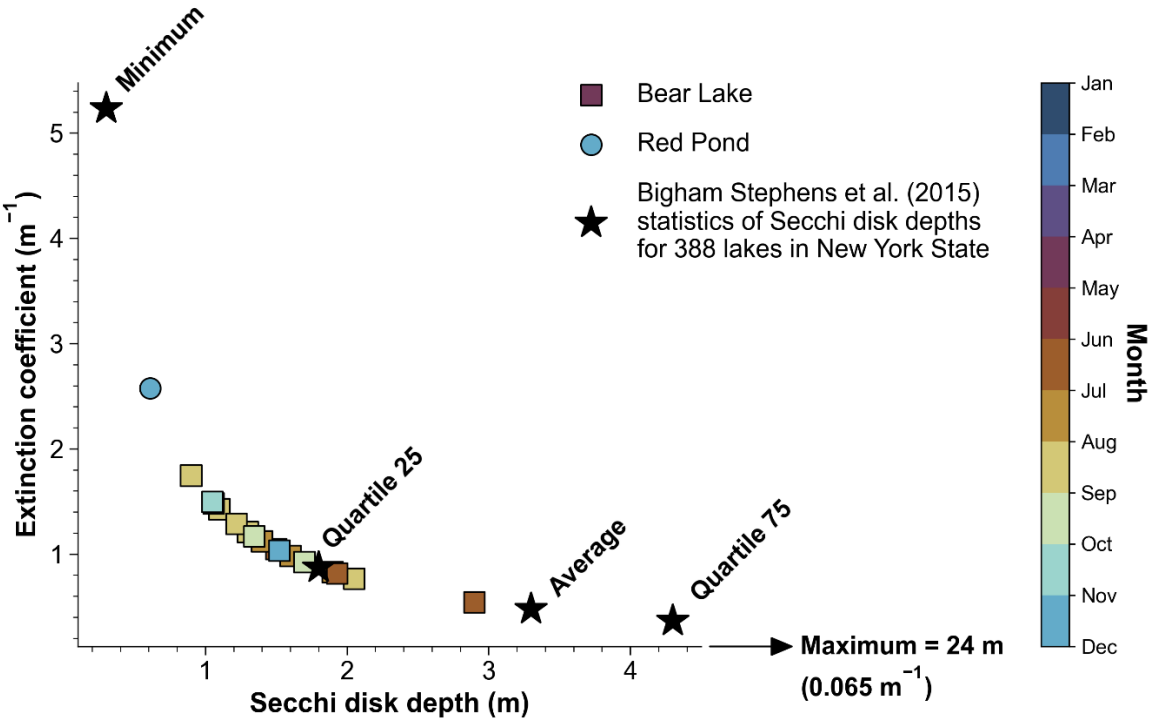

Figure S7. Observations of Secchi disk depth for Bear Lake (squares) and Red Pond (circle) colored by month. Bear Lake observations were collected as part of this study (n = 6) and supplemented with observations from the New York State Department of Environmental Conservation's Division of Water Monitoring Data Portal (n = 13; NYS DEC, 2025). Stars show the minimum, maximum, average, 25th quartile, and 75th quartile from a dataset of Secchi disk depths from 388 lakes in New York State (Bigham Stephens et al., 2015). Secchi disk depths were converted to light extinction coefficients using the formula $1.57/Z_{SD} = \eta$, where η is the light extinction coefficient in m-1 and Z_{SD} is the Secchi disk depth in m.

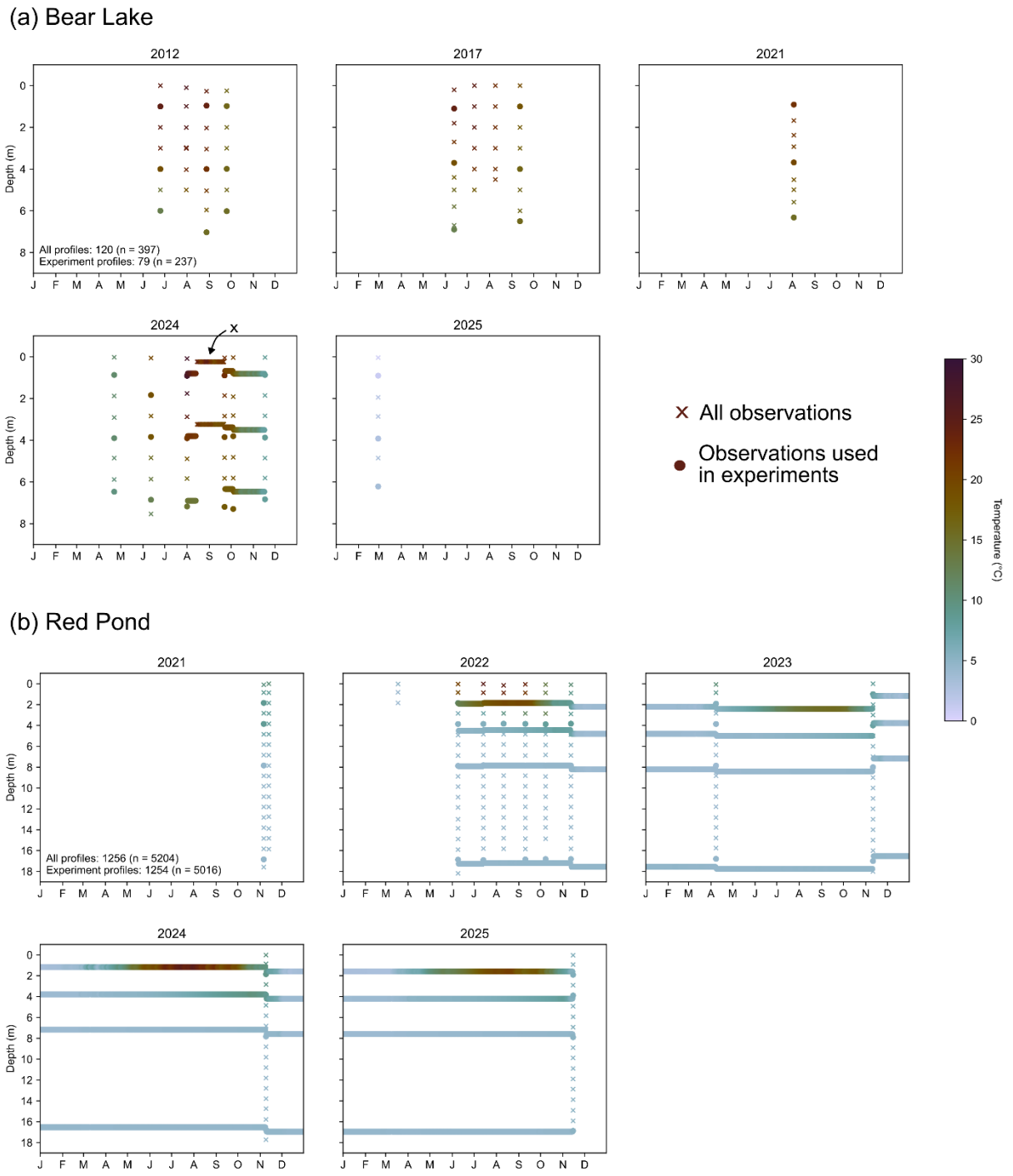

Figure S8. All lake water temperature observations and observations that make up profiles used in the experiments for (a) Bear Lake and (b) Red Pond. Dots are colored by water temperature value. The total number of profiles and number used in the experiments is shown in the first panel of (a) and (b), where n displays the number of individual data points included in the profiles.

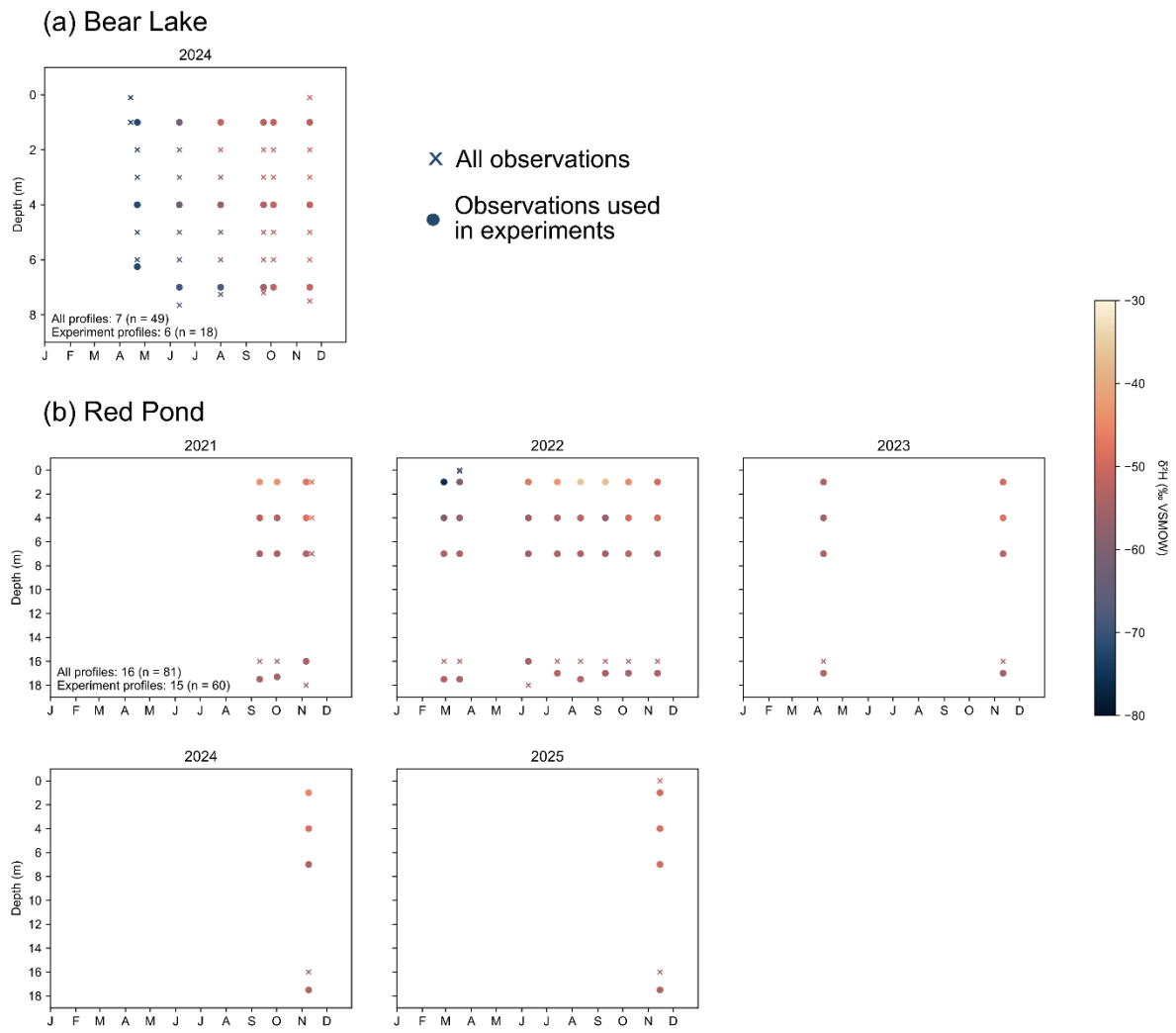

Figure S9. All lake water δ^2H observations (small dots) and observations that make up profiles used in the experiments (large dots) for (a) Bear Lake and (b) Red Pond. Dots are colored by water δ^2H value. The total number of profiles and number used in the experiments is shown in the first panel of (a) and (b), where n displays the number of individual data points included in the profiles.

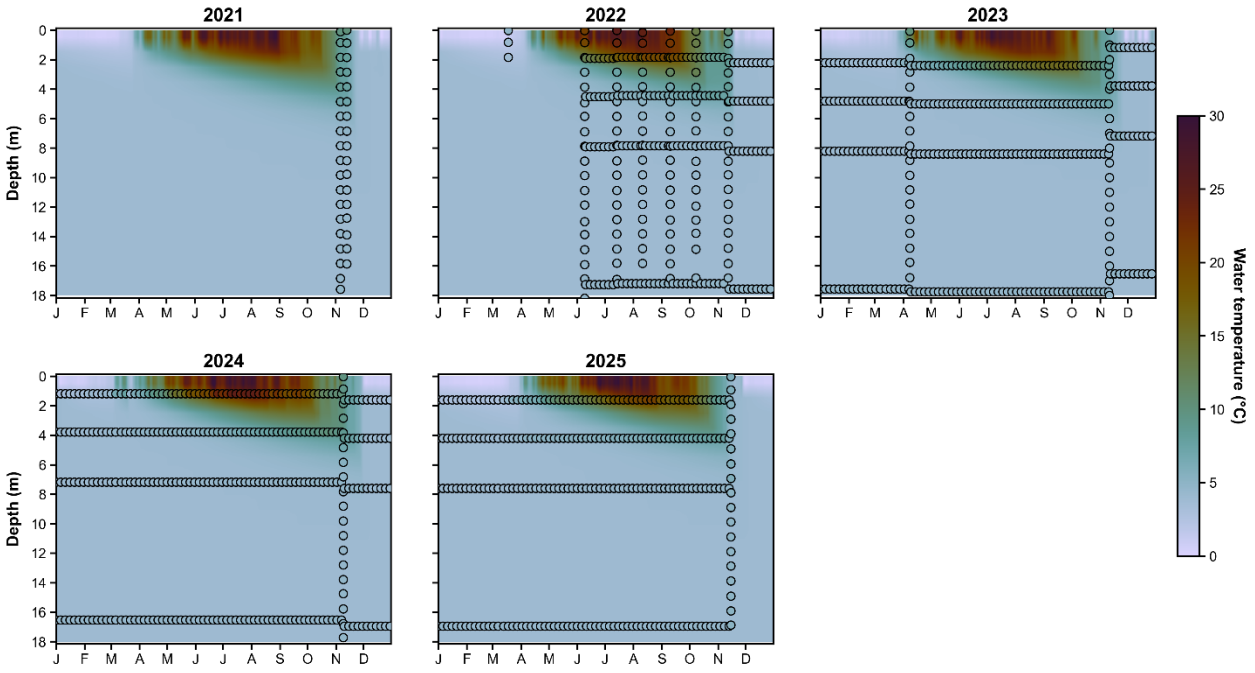

Figure S10. Results of environment submodel calibration to observed water temperature profiles from Red Pond. Colors are modeled ensemble averages for each day and depth. Dots are observations, colored by observed water temperature. For dense periods of daily observations, we plot every 5th measurement but calibrated to all measurements.

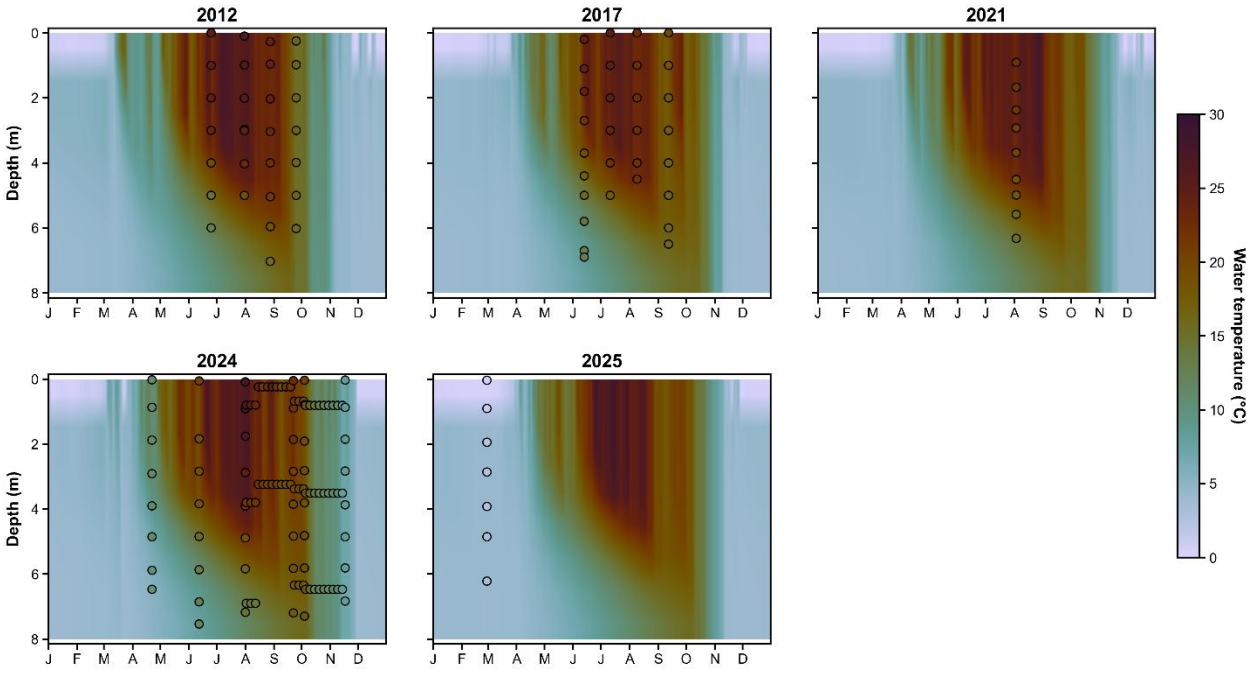

Figure S11. Results of environment submodel calibration to observed water temperature profiles from Bear Lake. Colors are modeled ensemble averages for each day and depths. Dots are observations, colored by observed water temperature. For dense periods of daily observations, we plot every 5th measurement but calibrated to all measurements.

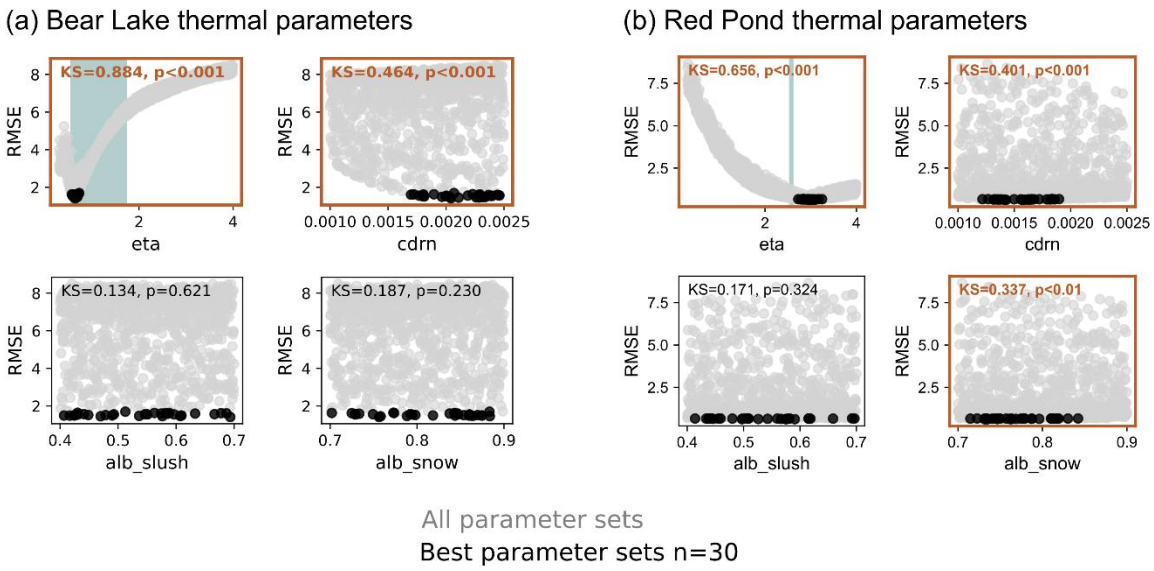

Figure S12. Parameter values and performance of each of the 1000 water temperature profile simulations for (a) Bear Lake and (b) Red Pond. Performance is measured as the root-mean-square error across all observations. Black dots are the 30 best-performing simulations calibrated to observations. Gray dots show the results for all 1000 simulations. To identify if the calibrated parameter ranges are significantly different from the uniform, original range, we use Kolmogorov-Smirnov (KS) tests and p-values. Subplots with orange text and outline highlight calibrated parameter distributions that are significantly different from the original range. In the 'eta' subplot, the blue line displays the value of estimated light extinction coefficient based on Secchi disk depth observations (Bear Lake: n = 19 and Red Pond: n = 1).

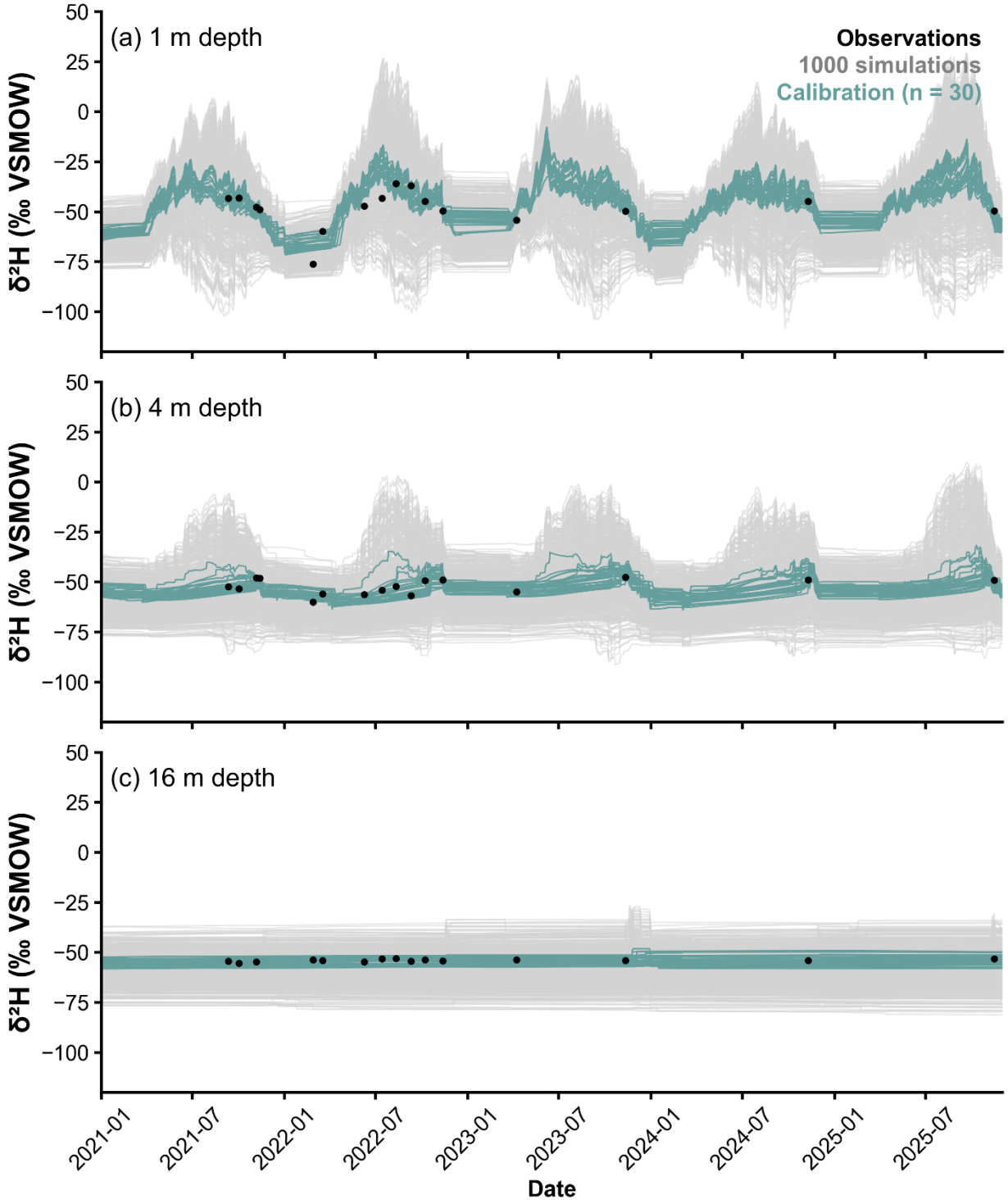

Figure S13. Results of environment submodel calibration to observed water δ^2H profiles from Red Pond. Panels show modeled and observed time series for selected depths: (a) 1 m, (b) 4 m, and (c) 16 m. Black dots are observations, blue lines are the best-performing simulations, and gray lines are all simulations.

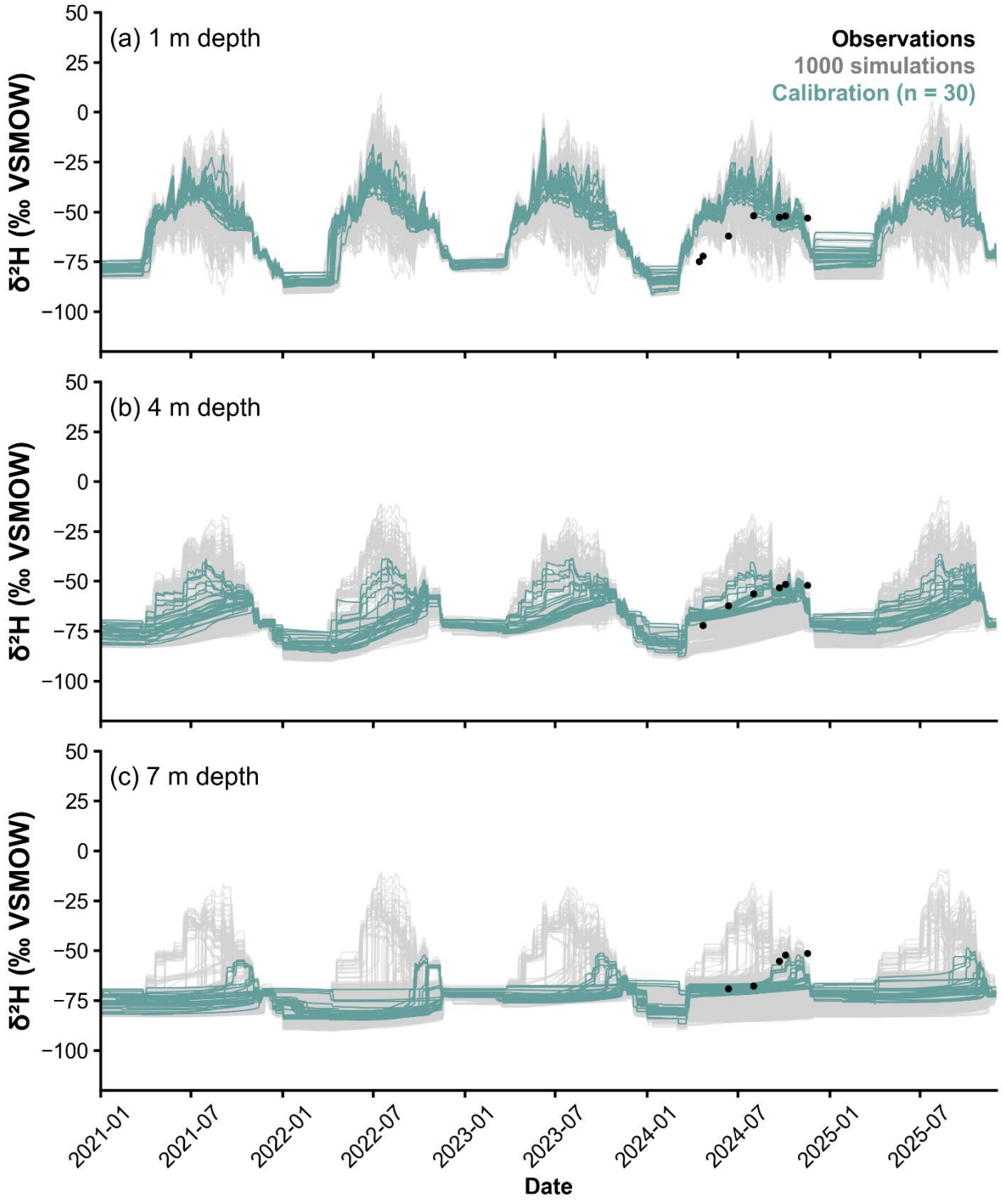

Figure S14. Results of environment submodel calibration to observed water δ^2H profiles from Bear Lake. Panels show modeled and observed time series for selected depths: (a) 1 m, (b) 4 m, and (c) 7 m. Black dots are observations, blue lines are the best-performing simulations, and gray lines are all simulations.

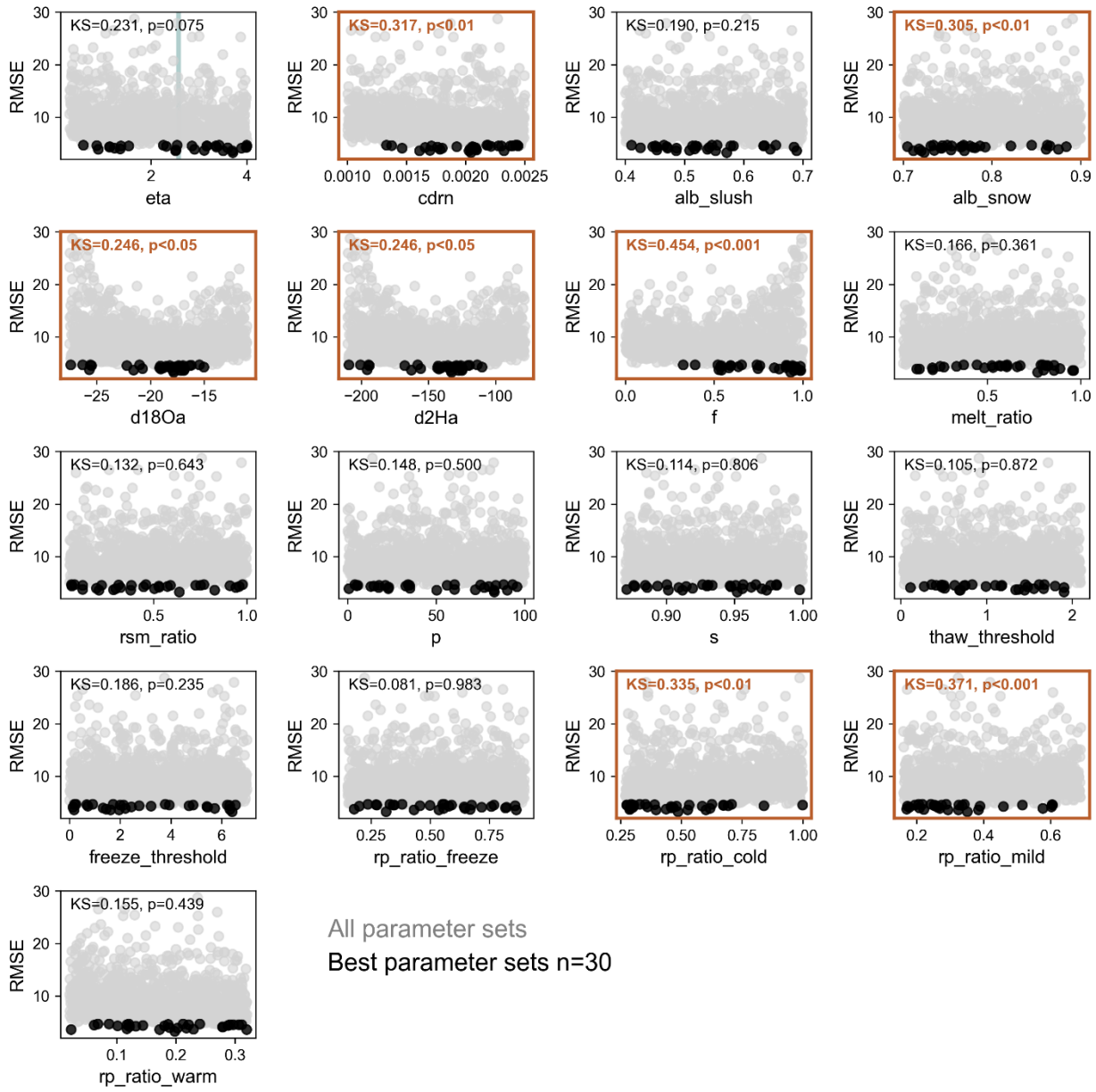

Figure S15. Parameter values and performance of each of the 1000 δ^2H profile simulations for Red Pond. Performance is measured as the root-mean-square error across all observations. Black dots are the 30 best-performing simulations calibrated to observations. Gray dots show the results for all 1000 simulations. To identify if the calibrated parameter ranges are significantly different from the uniform, original range, we use Kolmogorov-Smirnov (KS) tests and p-values. Subplots with orange text and outline highlight calibrated parameter distributions that are significantly different from the original range.

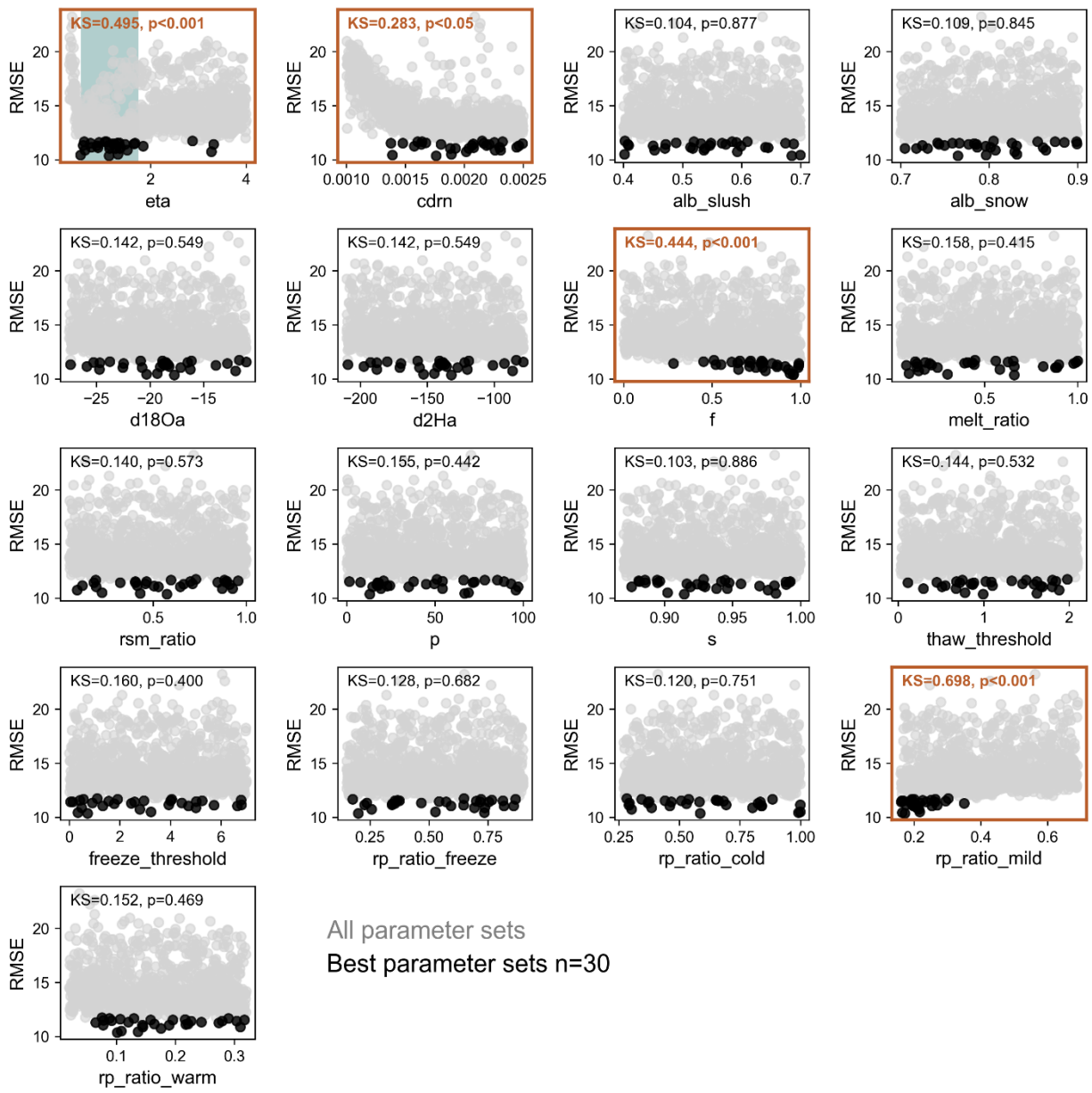

Figure S16. Same as Figure S15, but δ^2H profile simulations for Bear Lake calibrated to observations.

References

Bigham Stephens, D. L., Carlson, R. E., Horsburgh, C. A., Hoyer, M. V., Bachmann, R. W., and Canfield, D. E.: Regional distribution of Secchi disk transparency in waters of the United States, Lake and Reservoir Management, 31, 55–63, https://doi.org/10.1080/10402381.2014.1001539, 2015.

Corcoran, M. C., Thomas, E. K., and Boutt, D. F.: Event-Based Precipitation Isotopes in the Laurentian Great Lakes Region Reveal Spatiotemporal Patterns in Moisture Recycling, Journal of Geophysical Research: Atmospheres, 124, 5463–5478, https://doi.org/10.1029/2018JD029545, 2019.

Hersbach, H., Bell, B., Berrisford, P., Hirahara, S., Horányi, A., Muñoz-Sabater, J., Nicolas, J., Peubey, C., Radu, R., Schepers, D., Simmons, A., Soci, C., Abdalla, S., Abellan, X., Balsamo, G., Bechtold, P., Biavati, G., Bidlot, J., Bonavita, M., De Chiara, G., Dahlgren, P., Dee, D., Diamantakis, M., Dragani, R., Flemming, J., Forbes, R., Fuentes, M., Geer, A., Haimberger, L., Healy, S., Hogan, R. J., Hólm, E., Janisková, M., Keeley, S., Laloyaux, P., Lopez, P., Lupu, C., Radnoti, G., De Rosnay, P., Rozum, I., Vamborg, F., Villaume, S., and Thépaut, J.: The ERA5 global reanalysis, Q. J. R. Meteorol. Soc., 146, 1999–2049, https://doi.org/10.1002/qj.3803, 2020.

Hersbach, H., Bell, B., Berrisford, P., Biavati, G., Horányi, A., Muñoz Sabater, J., Nicolas, J., Peubey, C., Radu, R., Rozum, I., Schepers, D., Simmons, A., Soci, C., Dee, D., Thépaut, J-N.: ERA5 hourly data on single levels from 1940 to present, Copernicus Climate Change Service (C3S) Climate Data Store (CDS), [data set], https://doi.org/10.24381/cds.adbb2d47, 2023.

New York State Department of Environmental Conservation Division of Water: Division of Water Monitoring Portal (Version 1.27.2025) [data set], https://experience.arcgis.com/experience/301748017d7d40649bc5082fc1c5365e/#data_s=id%3AdataSource_1-1949977d66f-layer-14%3A1791, last access: 12 April 2025.

NOAA National Centers of Environmental Information: Global Surface Summary of the Day - GSOD. 1.0 [data set], https://www.ncei.noaa.gov/access/search/data-search/global-summary-of-the-day?pageNum=1&pageSize=100&bbox=42.734,-79.935,41.871,-78.411, last access: 14 March 2026, 1999.